

1 Mapping the causal chain from genetic risk 2 variants to lipid dysmetabolism in 3 Parkinson's disease

4 Ruth B. De-Paula,¹ Jonggeol Kim,² Herve Rhinn,³ Hiba Saade,² Fatima Chavez,² Téah
5 Segura,² Maria Valeria Lozano,² Michelle Etoundi,² Karla Silos,² Naomi Kass,² Viktoriya
6 Korchina,⁴ Harshavardhan Doddapaneni,⁴ Eric Venner,⁴ Joseph C. Masdeu,⁵ Valory Pavlik,²
7 Melissa M. Yu,² Chi-Ying R. Lin,² Joseph Jankovic,² Aron S. Buchman,^{6,7} Donna Muzny,⁴
8 Richard A. Gibbs,^{4,8} Sarah H. Elsea,^{4,8} Asa Abeliovich,³ Peter Lansbury,⁹ Nora Vanegas-
9 Arroyave,^{2,11} Chad A. Shaw^{8,10,11} and Joshua M. Shulman^{2,8,10,11,12}

10 Abstract

11 The molecular pathways linking genetic variants to Parkinson's disease (PD) onset and
12 progression remain incompletely defined; however, risk alleles in multiple genes, including
13 *GBA1*, strongly implicate lipid metabolism.

14
15 To systematically identify causal biomarker signatures, we analyzed comprehensive
16 metabolome profiles from blood plasma in 149 PD patients and 150 controls, along with
17 complementary genetic, RNA-sequencing, and metabolic data from other available clinical
18 and pathologic cohorts. Using colocalization and summary-data-based Mendelian
19 randomization, we tested whether expression and metabolic quantitative trait loci mediate
20 the association between implicated genetic variants and PD risk. We further integrated
21 differential metabolomics and proteomics from blood and brain to reveal pertinent
22 mechanisms.

23
24 We show that common PD risk variants at the *serine palmitoyltransferase small subunit B*
25 (*SPTSSB*) locus, a key regulator of *de novo* sphingolipid biosynthesis, are associated with
26 increased *SPTSSB* brain expression and elevated plasma ceramides. Additional analyses
27 strongly support our hypothesis that a common *SPTSSB* causal variant is responsible for
28 PD risk as well as the expression and metabolic quantitative trait loci. Multiple

1 sphingolipids and fatty acid derivatives were perturbed in PD, and we identified both
2 unique and shared features with the Alzheimer's disease metabolome. A PD acylcarnitine
3 signature was further replicated in human postmortem brain tissue, when comparing those
4 with or without preclinical Lewy body pathology. Integrated analysis of complementary
5 brain proteomic profiles revealed dysregulation of mitochondrial processes dependent on
6 acylcarnitines, including fatty acid beta-oxidation, the tricarboxylic acid cycle, and
7 oxidative phosphorylation.

8
9 Our results identify promising biomarkers and reveal a causal chain linking genetic
10 variation to altered gene/protein expression, lipid dysmetabolism, and the manifestation of
11 PD.

12

13 **Author affiliations:**

14 1 Quantitative and Computational Biosciences Program, Baylor College of Medicine,
15 Houston, TX 77030, USA

16 2 Department of Neurology, Baylor College of Medicine, Houston, TX 77030, USA

17 3 Leal Therapeutics, Worcester, MA, USA

18 4 Human Genome Sequencing Center, Baylor College of Medicine, Houston, TX 77030,
19 USA

20 5 Nantz National Alzheimer Center, Houston Methodist Neurological Institute and Weill
21 Cornell Medicine, Houston, TX 77030, USA

22 6 Rush Alzheimer's Disease Center, Rush University Medical Center, Chicago, IL 60612,
23 USA

24 7 Department of Neurological Sciences, Rush University Medical Center, Chicago, IL
25 60612, USA

26 8 Department of Molecular and Human Genetics, Baylor College of Medicine, Houston, TX
27 77030, USA

28 9 Department of Neurology, Harvard Medical School, Boston, MA 02115, USA

29 10 Jan and Dan Duncan Neurological Research Institute, Texas Children's Hospital,
30 Houston, TX 77030, USA

1 11 Center for Alzheimer's and Neurodegenerative Diseases, Baylor College of Medicine,
2 Houston, TX 77030, USA

3 12 Department of Neuroscience, Baylor College of Medicine, Houston, TX 77030, USA

4
5 Correspondence to: Joshua M. Shulman, MD, PhD

6 Jan and Dan Duncan Neurological Research Institute

7 1250 Moursund St.

8 Houston, TX 77030, USA

9 E-mail: Joshua.Shulman@bcm.edu

10

11 **Running title:** Causal chain and lipid dysmetabolism in PD

12 **Keywords:** *SPTSSB*; *GBA1*; sphingolipids; acylcarnitine; fatty acid; Lewy body

13

14 Introduction

15 More than 100 susceptibility loci have been discovered for Parkinson's disease (PD);
16 however, a major gap exists to understand how implicated genetic risk variants lead to the
17 development of alpha-synuclein pathology and initial clinical manifestations of the
18 disease^{1,2}. Loss-of-function variants in the *Glucocerebrosidase* (*GBA1*) gene are among the
19 most common and potent PD genetic risk factors, conferring at least 5-fold increased risk
20 for PD³. *GBA1* encodes the lysosomal enzyme responsible for breakdown of
21 glucosylceramide, a key precursor for membrane sphingolipids⁴. Common or rare variants
22 in other genes encoding lysosomal enzymes or cofactors regulating metabolism of
23 ceramides and sphingolipids have similarly been linked to PD risk (e.g. *SCARB2*, *ARSA*,
24 *SMPD1*, and *GALC*) (**Figure 1A**)⁵⁻⁹. Based on studies in animal and cellular models,
25 disruption of lysosomal metabolism and the accumulation of undigested sphingolipid
26 species may directly promote alpha-synuclein pathology¹⁰⁻¹². Thus, perturbations in
27 sphingolipid/ceramide metabolism are a promising candidate mechanism by which
28 genetic variants may drive PD clinical and pathologic manifestations^{13,14}.

29 Prior to the appearance of cardinal motor signs, individuals with PD progress
30 through preclinical and prodromal phases characterized by absent or minimal symptoms

1 in association with brain pathology, making the discovery of sensitive biomarkers for early
2 detection and monitoring of disease progression a priority¹⁵. Published studies in blood,
3 CSF, and postmortem brain tissue suggest perturbations in sphingolipids as well as other
4 lipid metabolites—or changes in the activity of enzymes like Glucocerebrosidase—may
5 accompany PD^{16–23}. However, interpretation of these studies to infer early or proximal,
6 causal changes is challenging since most studies do not control for disease duration, and
7 sphingolipid perturbations may also be a downstream consequence of PD
8 pathophysiology. Indeed, a preponderance of experimental data demonstrate that alpha-
9 synuclein pathology can feedback to disrupt lysosomal function and lipid metabolism^{11,12}.
10 Beyond the lysosome, mitochondrial dysfunction has also been implicated in PD
11 pathogenesis, and mitochondria are a critical hub for metabolism, participating in fatty
12 acid catabolism and oxidative phosphorylation^{1,24,25}. Integration of genetic and metabolic
13 markers may be a promising strategy both to identify biomarkers and resolve causal
14 pathways. For example, in a recent large study integrating genotyping and cerebrospinal
15 fluid metabolomics, common genetic variants in *arylsulfatase A (ARSA)* were associated
16 with both PD risk and tyrosine derivatives from cerebrospinal fluid (CSF)²⁶. Another
17 challenge to robust PD biomarker discovery stems from the common co-occurrence of
18 other age-related brain pathologies²⁷, such as Alzheimer’s disease, which may interact with
19 PD pathology and potentially cause related metabolic changes²⁸.

20 We have comprehensively profiled metabolism in 398 individuals (149 PD cases, 99
21 AD cases, and 150 controls) and analyzed together with genetic data on *GBA1* and related
22 lysosomal genes. We integrated these results with complementary analysis of available
23 genetic, metabolic, and proteomic data from additional cohorts, including from blood ($n =$
24 4,492; $n = 19,994$) and postmortem brain tissue ($n = 429$), identifying promising biomarkers
25 of lipid dysmetabolism in PD / Lewy body pathology. Our results further highlight a causal
26 chain between risk variants at the *SPTSSB* locus, encoding a subunit of serine palmitoyl
27 transferase (SPT), which drive increased sphingolipid production and altered fatty acid
28 metabolism, leading to elevated PD risk.

29

30 Materials and methods

31 Human Subjects

32 Human subject studies were conducted in accordance with the Declaration of Helsinki.
33 Institutional review boards at Baylor College of Medicine (BCM) and the Houston Methodist
34 (HM) approved both the biospecimen collection and sequencing (H-50254; PRO00034371).

1 Subjects were recruited from the BCM Parkinson's Disease Center and Movement
2 Disorders Clinic and Alzheimer's Disease and Memory Disorders Clinic and from the HM
3 Nantz National Alzheimer Center between 2022-2024. Patients with PD and Alzheimer's
4 disease were diagnosed by neurologists with subspecialty training in movement or memory
5 disorders, respectively. Unrelated controls were screened to exclude individuals with
6 potential PD symptoms or those having a first-degree family history of PD or dementia.

7 We also leveraged published clinical, pathologic, demographic, genome/RNA
8 sequencing, proteomics, and metabolic profile data from the Religious Orders Study and
9 Rush Memory and Aging Project (ROSMAP). All ROSMAP participants enrolled without
10 known dementia and agreed to detailed clinical evaluation and brain donation at death²⁹.
11 The ROSMAP studies were approved by the Institutional Review Board at Rush University
12 Medical Center (ROS IRB# L91020181, MAP IRB# L86121802). Each participant signed an
13 informed consent, Anatomic Gift Act, and an RADC Repository consent (IRB# L99032481)
14 allowing data and biospecimens to be repurposed. For the analyses of differential
15 metabolism and protein expression, Lewy body cases were classified based on alpha-
16 synuclein positive Lewy body pathology in the substantia nigra, neocortex, and/or limbic
17 area (variable: *dlbany*)³⁰, and AD pathologic diagnosis was based on high or intermediate
18 likelihood of AD according to NIA-Reagan scores (variable: *niareagansc*)^{31,32}. ROSMAP
19 single nucleus transcriptomes from dorsolateral prefrontal cortex tissues includes RNA-
20 sequencing from 436,014 excitatory and 159,838 inhibitory neurons³³.

21

22 Genome Sequencing

23 For BCM/HM samples, DNA was extracted from peripheral blood cells using the E.Z.N.A.
24 SQ Blood DNA Kit (Omega Bio-tek Inc.) or from saliva samples using the Gentra Puregene
25 Blood Kit (QIAGEN). The BCM Human Genome Sequencing Center followed published
26 library preparation and sequencing protocols³⁴ using the Illumina NovaSeq 6000 platform
27 and S4 flow cells to generate 150 bp paired-end reads. Sequence data was aligned to
28 hg38³⁵ followed by variant calling using the Illumina DRAGEN software, v3.7.8³⁶. An R
29 pipeline was used to extract all single nucleotide variants (SNVs) within multi-sample
30 Variant Call Files (VCFs). For the *SPTSSB* analyses, we interrogated *rs1450522* (hg38
31 chr3:161,359,842 A>G), based on published PD genome-wide association studies⁵. For
32 *GBA1*, we queried the well-established PD risk variants, L444P, N370S, T369M, and
33 E326K^{37,38}.

34

1 Metabolomics

2 Global metabolomics (Metabolon HD4 platform) intensity values, representing the area
3 under the curve of mass-spectrometry peaks proportional to metabolite abundance, were
4 generated and batch corrected, as previously described²⁸. In total, 1,409 plasma
5 metabolites were detected from plasma (BCM/HM), and 1,055 metabolites from brain
6 (ROSMAP dorsolateral prefrontal cortex). As in prior work³⁹, metabolites with >30% missing
7 values were excluded, resulting in 1,171 plasma and 685 brain metabolites for analysis.
8 The remaining missing values were imputed as minimum. Data were log-transformed and
9 mean centered as z-scores.

10

11 Analysis of differential metabolites

12 A likelihood-ratio test (LRT) was used to assess metabolic dysregulation in plasma
13 comparing PD cases with controls. Linear regression models were constructed for each
14 metabolite and used to calculate LRT statistics using R⁴⁰, comparing a full model
15 (metabolite ~ PD + age + sex) with a reduced model (metabolite ~ age + sex). Residuals of
16 reduced models were used for plotting and downstream analyses. To adjust for multiple
17 hypothesis testing, we applied the Benjamini-Hochberg False Discovery Rate (FDR), using
18 a q-value < 0.05 to establish significance. Volcano plots were generated using the R
19 package *ggplot2* (v. 3.4.4)⁴¹. To address specificity, the identical workflow was used to
20 identify blood metabolic perturbations in Alzheimer's disease. Venn diagrams were
21 calculated using *nVenn*, and we performed a Fisher test to assess overlap significance. The
22 background of metabolites was the total number of all molecules included for the
23 differential metabolic analysis.

24 We performed additional secondary analyses in the BCM/HM clinical cohort to
25 address the sex imbalance between cases and controls. We first used nearest-neighbor
26 multivariate matching to generate a balanced cohort of 97 PD cases and 97 controls.
27 Subject pairs were defined using the R package *Matching* (v. 4.10.15), with default
28 parameters⁴². A distance score was calculated for each pair using the absolute difference
29 in age summed with the absolute difference in sex (1 = female; 2 = male) times 10. Only
30 subjects with distance score < 10 (exact sex match) were included, resulting in 97 paired
31 (54 females and 43 males) PD cases and Controls. Clinical and demographic details are
32 available in **Supplemental Table 1**. A Wilcoxon signed-rank test was implemented for
33 significance testing. As an alternate approach, we also performed a stratified analyses in
34 which males (94 cases / 50 controls) and females (55 cases / 100 controls) were
35 considered separately.

1 LRT was also implemented for the analysis of brain metabolic perturbations in
2 ROSMAP. We included a covariate for postmortem interval (PMI), comparing a full model
3 (metabolite ~ Lewy body pathology + age + sex + PMI) with a reduced model (metabolite ~
4 age + sex + PMI). For the metabolome-wide analysis, we again applied an FDR significance
5 threshold (q -value < 0.05). For replication of PD-associated acyl carnitine changes and the
6 analysis of class-wide metabolite perturbations, we relaxed the threshold and considered
7 an unadjusted p -value < 0.05 .

8 9 Quantitative trait locus analysis

10 For single variant analyses, boxplots of metabolite normalized residuals (corrected for age
11 and sex) were plotted using the R package *ggplot2* (v. 3.4.4)⁴¹. Additive and recessive linear
12 models (corrected for age and sex) tested the association of *SPTSSB*^{rs1450522} on levels of
13 sphingolipids and ceramides. For these secondary analyses, we considered an unadjusted
14 $p < 0.05$ denoting a suggestive level of significance. We also assessed significance
15 (*fisher.test* in R) of class-wide enrichment of associations among all sphingolipids in the
16 BCM cohort (8 out of 62 sphingolipids versus 64 out of 1,171 total metabolites) and Cadby
17 et al.⁴³ cohort (15 out of 126 sphingolipids versus 22 out of 595 total lipids). A similar
18 analysis examined the enrichment for associations among fatty acids in the Surendran et
19 al.⁴⁴ cohort (19 out of 68 fatty acids versus 65 out of 911 total metabolites).

20 Colocalization analysis was performed using *coloc* in R⁴⁵ and hg19 genome build,
21 adopting a published pipeline^{6,46}. PD GWAS summary statistics⁴⁷ were extracted for
22 variants from the *SPTSSB* locus (± 500 kb), along with eQTL / mQTL data (GTEX⁴⁸,
23 BrainMeta⁴⁹, and OmicScience^{44,50}). Besides *SPTSSB*, secondary analyses considered
24 eQTLs for other locus candidates (*PPML1*, *B3GALNT1*, *NMD3* and *OTOL1*). We considered
25 posterior probabilities (PP), including PP.H3, representing the probability that both traits
26 (PD risk / QTL) are associated but have independent causal variants, and PP.H4, for the
27 probability that the traits share a common causal variant. Co-localization was considered
28 significant if $PP.H4 > 0.8$ and $PP.H4 > PP.H3$.

29 Summary-data-based Mendelian Randomization (SMR) was implemented following
30 published methods⁴⁹ using the same summary statistics as for co-localization. Genetic
31 instruments were constructed using significant variants ($p < 5 \times 10^{-8}$), without clumping
32 (variants were in strong LD). Each mQTL was annotated to the gene most closely localized
33 to the variant. SMR and HEterogeneity In Dependent Instruments (HEIDI) horizontal
34 pleiotropy analysis was performed using SMR version 1.3.1. eQTL formatted input files
35 (BESD/ESI/EPI) were obtained online

1 (<https://yanglab.westlake.edu.cn/software/smr/#DataResource>). mQTL summary statistics
2 were converted to BESD format using `--matrix-eqtl-format` and `--make-besd` flags. ESI files
3 were annotated to include chromosome, position, effect allele, other allele, and effect
4 allele frequency. EPI files were similarly annotated to include chromosome, probe name,
5 central gene position, gene name, and gene strand for all genes within the *SPTSSB* LD
6 locus. Finally, SMR and HEIDI tests were run using `--bfile` for defining PLINK 1000 Genomes
7 European reference binaries; `--beqtl-summary` and `--gwas-summary` flags for defining QTL
8 and GWAS inputs, respectively; `--peqtl-smr 0.05` and `--peqtl-heidi 0.05` for defining
9 statistically significant QTLs; and `--smr-multi` for defining a multi-SNP analysis. We used
10 SMR and SMR MultiSNP $p < 0.05$ to define SNP and locus significance, respectively, and
11 HEIDI $p > 0.05$ to define absence of pleiotropy.

12

13 Proteomics

14 ROSMAP proteomic data was based on untargeted, tandem mass tag mass spectrometry
15 from dorsolateral prefrontal cortex tissue⁵¹. We excluded peptides with >30% missing
16 values; the remaining missing values were imputed as minimum. Peptide abundances
17 mapping to the same protein were summed, resulting in 7,596 proteins. Data were log-
18 transformed and mean-centered as z-scores. For differential expression analysis, LRT were
19 implemented as described above. Overrepresentation analysis was implemented in
20 MetaScape (<https://metascape.org/gp/index.html>)⁵². To identify dysregulated proteins, we
21 used an unadjusted $p < 0.05$, and FDR < 0.05 was used as the significance threshold for
22 identification of enriched pathways. Background was set for the total number of proteins
23 detected.

24

25 Results

26 PD risk variant at *SPTSSB* associates with sphingolipid and fatty acid 27 changes in blood

28 Common or rare variants in several genes, including *GBA1*, strongly implicate sphingolipid
29 and ceramide metabolism in PD risk and pathogenesis (**Figure 1A**). We generated
30 comprehensive metabolic profiles from blood (plasma) in 149 PD cases and 150
31 neurologically-healthy controls. PD cases had a mean age of 65.3 years (range 34-85), were
32 36.9% female, and had a mean disease duration of 8 years (**Supplemental Table 1**).

1 Overall, we identified 62 sphingolipid and ceramide species, of which 14 (23%) showed
2 significant PD-associated perturbations in blood (FDR < 0.05) based on analyses adjusted
3 for age and sex, (**Figure 1B**, **Supplemental Figure 3**, and **Supplemental Data 1**).
4 Interestingly, smaller ceramide precursors (e.g., dihydroceramide) were down-regulated in
5 PD, whereas more complex sphingolipids were predominantly up-regulated (7 out of 8
6 metabolites, including glucosylceramide and lactosylceramide). Our results are consistent
7 with prior studies showing sphingolipid perturbations in PD²⁰. Since our case and control
8 cohort composition differed by sex, we repeated the analysis using nearest-neighbor
9 matching to create a smaller but more balanced cohort of 97 PD cases and 97 controls: 10
10 out of 14 sphingolipid species remained significantly dysregulated among PD cases
11 (**Supplemental Data 1**).

12 To differentiate proximal, causal changes from downstream metabolic feedback
13 resulting from PD pathogenesis, we performed secondary analyses restricted to controls
14 without PD and further stratified the sample based on the presence of PD risk variants in
15 genes that regulate sphingolipid/ceramide synthesis or breakdown (**Figure 1A**). *GBA1*
16 variants are uncommon in our sample (only 9 PD cases and 6 controls), limiting statistical
17 power to interrogate for differential metabolic signatures. Similarly, rare loss-of-functions
18 variants in *SMPD1* or *ARSA*, which are also established to increase PD risk⁷⁻⁹, were not
19 present in our dataset. We next considered common risk variants identified from PD
20 genome-wide association studies^{5,47}, including *rs28628748* (freq. = 0.37) in *SCARB2*,
21 encoding a chaperone required for *GBA1* transport to the lysosome, and *rs979812* (freq. =
22 0.44) at the *GALC* locus, which is linked to the lysosomal storage disorder, Krabbe disease.
23 However, neither of these variants were associated with sphingolipid perturbations in our
24 data.

25 Though not as well studied as *GBA1* and other lysosomal genes, a genome-wide
26 significant association (*rs1450522*^G, freq. = 0.31, odds ratio ~ 1.1) has also been reported^{5,47}
27 at the *serine palmitoyltransferase small subunit B (SPTSSB)* locus, encoding a regulatory
28 subunit of SPT, which participates in the initial, rate-limiting reaction for *de novo*
29 sphingolipid synthesis. The SPT complex catalyzes the condensation of serine with a fatty
30 acid derivative, usually palmitoyl-CoA, to generate 3-ketosphinganine (also known as 3-
31 ketodihydrosphingosine)⁵⁴. Interestingly, besides the association of common *SPTSSB*
32 variants with PD risk, rare gain-of-function mutations in genes encoding other SPT subunits
33 have been identified as causes of hereditary sensory and autonomic neuropathy type 1
34 (*SPTLC1* and *SPTLC2*), hereditary spastic paraplegia (*SPTSSA*), and amyotrophic lateral
35 sclerosis / frontotemporal dementia (*SPTLC1* and *SPTLC2*)^{14,55-58}. Among neurologically
36 healthy controls in our local cohort, we identified 60 heterozygous and 9 homozygous
37 carriers of the *SPTSSB*^{*rs1450522-G*} PD risk allele, along with 79 non-carriers. We discovered that

1 the *SPTSSB* variant was, in fact, suggestively associated with changes in 8 out of 62
2 assayed sphingolipids and ceramides in our dataset, including 4 out of the 14 sphingolipids
3 altered in PD (above) (**Figure 1C, Supplemental Figure 5, Supplemental Table 3**). When
4 compared with other metabolites interrogated from plasma, there was evidence of a
5 significant class-wide enrichment for associations between *SPTSSB*^{rs1450522} with
6 sphingolipids and ceramides ($p = 0.016$). Notably, elevated plasma levels for
7 glucosylceramide, lactosylceramide and multiple sphingomyelin species were observed
8 among those with the *SPTSSB*^{rs1450522-G} PD risk allele. For selected sphingomyelin and
9 glucosyl ceramide species, the association appeared to be driven by the *SPTSSB*^{rs1450522-G}
10 homozygote class. Among PD cases, the association was further enhanced, such that
11 *SPTSSB*^{rs1450522-G} was associated with perturbations in 16 out of 62 sphingolipids
12 (**Supplemental Table 3 and Supplemental Figure 4**). Our results are potentially consistent
13 with a metabolic quantitative trait locus (mQTL), linking *SPTSSB* genetic variation with
14 increased sphingolipid production.

15 To further replicate the association between the *SPTSSB* variant and elevated
16 sphingolipids, we leveraged available plasma lipidomics or metabolomics along with
17 genotyping data from other published studies. We first considered data from an Australian
18 cohort ($n = 4,492$) without known neurological disease⁴³. Strikingly, among 595 lipid
19 species interrogated, the top-ranked associations with the *SPTSSB*^{rs1450522-G} PD risk allele
20 are significantly enriched for sphingolipids ($p = 1.7 \times 10^{-6}$), including suggestive increases in
21 multiple ceramides [e.g., d20:1/24:0; d20:1/24:1], dihydroceramide [d18:0/18:0], as well as
22 sphingomyelin species (**Figure 1D and Supplemental Data 3**). Consistent with increased
23 *de novo* sphingolipid synthesis, we also discovered a suggestive association with elevated
24 sphinganine levels (unadjusted $p = 0.025$) in a large European cohort ($n = 19,994$ healthy
25 individuals)⁴⁴. Sphinganine is only two steps away from the reaction catalyzed by the SPT
26 enzymatic complex (**Figure 1A**). Of note, only 23 sphingolipids and no ceramides were
27 included in this European dataset. Lastly, to determine other candidate metabolic markers
28 for *rs1450522* carriers, we interrogated all 301 lipids detected in this larger and more
29 powerful cohort. Interestingly, fatty acids were significantly enriched for perturbations
30 among *rs1450522* carriers (19 out of 65 species affected, $p = 2.9 \times 10^{-8}$). Among this group,
31 *SPTSSB*^{rs1450522-G} was suggestively associated with reduced levels of the fatty acid,
32 heptanoate (unadjusted $p = 6 \times 10^{-4}$). Notably, fatty acids are important for sphingolipid
33 synthesis, and the SPT substrate and fatty acid derivative, palmitoyl-CoA, is also a key
34 building block and regulator of fatty acid synthesis^{14,25}. We also found that the levels of
35 selected sphingolipids and free fatty acids were correlated in both blood and brain tissue
36 (**Supplemental Figures 10-11 and Supplemental Data 1**).

37

1 PD risk variants colocalize with *SPTSSB* expression in brain and fatty acid 2 perturbations in blood

3 The lead PD risk variant at *SPTSSB*, *rs1450522*^G, is located within the 5'-untranslated region
4 (UTR), suggesting a potential impact on mRNA processing and/or stability. Consistent with
5 this, an *SPTSSB* expression quantitative trait locus (eQTL) was previously reported as part
6 of systematic follow-up analyses from the genome-wide association study discovering this
7 PD risk locus^{5,59}. To further investigate the relation between *rs1450522* and *SPTSSB* mRNA
8 expression we leveraged several complementary datasets pairing genotyping and RNA-
9 sequencing (RNA-seq). In the Genotype-Tissue Expression Portal (GTEx)⁴⁸ and BrainMeta⁴⁹
10 datasets, we confirmed that *rs1450522*^G is associated with increased *SPTSSB* expression in
11 both bulk human brain and tibial nerve tissue (**Supplemental Figure 1A**). We also
12 interrogated a single nucleus expression dataset from the Religious Orders Study and Rush
13 Memory and Aging Project (ROSMAP)³³ postmortem dorsolateral pre-frontal cortex tissue,
14 highlighting a significant *SPTSSB* eQTL present in excitatory and inhibitory neurons, but not
15 glia (**Supplemental Figure 1B-C, Supplemental Table 4**)⁶⁰. The association was strongest
16 in excitatory neurons, highlighting a potential dose-dependent relationship between the
17 *rs1450522*^G variant and *SPTSSB* mRNA levels ($p = 8.1 \times 10^{-32}$).

18 Together, our results show that *rs1450522*^G is not only associated with PD risk, but
19 also is related with both increased *SPTSSB* expression and altered metabolism affecting
20 multiple sphingolipids, fatty acids, and derivatives. To further examine the potential causal
21 chain between *SPTSSB* genetic variation, gene expression, metabolism, and PD (**Figure**
22 **2A**), we next performed complementary analyses using colocalization followed by
23 summary-data-based mendelian randomization (SMR) to examine for consistent,
24 correlated and causal associations between genetic variation at the *SPTSSB* locus and the
25 pertinent eQTL and mQTLs detected above (**Figure 2B, Table 1, Supplemental Table 5,**
26 **Supplemental Data 3**). For optimal statistical power, we leveraged updated genome-wide
27 association study summary statistics from the Global Parkinson's Disease Genetics
28 consortium (GP2)⁴⁷, incorporating results from 64,047 PD cases and 1,754,191 controls.
29 We primarily focused on the cell-type specific brain eQTL from excitatory neurons and the
30 plasma heptanoate mQTL, comprising the most robust associations from our analyses of
31 *SPTSSB*^{*rs1450522-G*}.

32 We discovered significant colocalization between the association signal for PD
33 genetic risk at the *SPTSSB* locus with either *SPTSSB* mRNA expression in excitatory neurons
34 and plasma heptanoate levels [posterior probability (PP.H4) of 97% and 89% respectively],
35 and similar results are seen for a direct comparison between *SPTSSB* eQTL and plasma
36 heptanoate (PP.H4 = 90%) (**Figure 2 and Supplemental Figure 6**). Consistent results were

1 also independently obtained using SMR (**Table 1** and **Supplemental Data 3**). Overall, our
2 results provide strong support for the hypothesis that the 3 traits (PD, excitatory neuron
3 *SPTSSB* eQTL, heptanoate mQTL) share a common causal variant, consistent with a
4 molecular cascade from genetic variation at *SPTSSB* to increased mRNA expression,
5 altered metabolism, reduced plasma heptanoate levels, and PD susceptibility. In addition,
6 we obtained consistent, albeit somewhat attenuated results when using dorsolateral
7 prefrontal cortex bulk tissue instead of the single-nucleus expression profiles from
8 excitatory neurons (**Table 1, Supplemental Figure 7, Supplemental Data 3**). However, it
9 was not possible to robustly model the causal pathway within a single tissue compartment
10 (i.e., brain or blood) (**Supplemental Figure 1A**). Interestingly, in data from one recent
11 published analysis²⁶, we did find a modest association ($p = 0.035$) between *SPTSSB*^{rs1450522-G}
12 and increased glucosylceramide in cerebrospinal fluid. Lastly, we also considered other
13 candidate genes at the susceptibility locus defined by *rs1450522* (**Supplemental Data 3**).
14 Besides *SPTSSB* and consistent with published results^{5,59,61}, we also confirmed an eQTL for
15 the adjacent gene, *NMD3*, which was present in blood and bulk cortical brain tissue but not
16 excitatory neurons. *NMD3* regulates RNA processing and is not known to have a role in lipid
17 metabolism. Other nearby genes, including *PPM1L*, *B3GALNT1*, and *OTOL1*, did not show
18 any evidence for an eQTL.

19

20 PD is characterized by fatty acid and acylcarnitine perturbations in blood

21 The preceding analyses highlight how sphingolipids and other fatty acid species might
22 serve as both PD biomarkers and causal mediators, linking genetic risk variants to disease
23 manifestations. In order to systematically define other promising PD signatures, we next
24 conducted a metabolome-wide analysis, interrogating 1,171 metabolites from blood
25 plasma (**Supplemental Figure 2**) among our PD case/control cohort. Overall, we identified
26 196 metabolites that survived multiple testing correction ($FDR < 0.05$), including 52
27 increased and 144 decreased species (**Figure 3A-B, Table 2, Supplemental Data 1**). Most
28 metabolite perturbations were consistent when the analysis was repeated in the smaller
29 but more balanced, sex-matched cohort (**Table S7 and Supplemental Data 1**). The most
30 extreme, PD-associated metabolic perturbations in blood, are well-known breakdown
31 products of levodopa⁶², including 3-methoxytyrosine, vanillactate, 3-methoxytyramine
32 sulfate, and other tyrosine derivatives (**Figure 3A**). Alterations in plasma lipids were the
33 second-most common among all PD-associated metabolic changes (37 out of all 196
34 differential metabolites), possibly due to the disproportionate representation of this class
35 in our assay panel (**Figure 3C, Supplemental Figure 2**). As expected, the sphingolipid
36 pathway was enriched for PD-associated changes (**Figure 3D**). Behenoyl-

1 dihydrosphingomyelin was one of the top-ranked downregulated species in the PD
2 metabolome, with a mean 0.71-fold decrease in PD plasma (FDR = 2.05×10^{-9}).

3 We also detected PD-associated plasma perturbations in several phospholipids (3
4 increased / 5 decreased), free fatty acids (2 increased / 7 decreased), and acylcarnitines (5
5 decreased). Although heptanoate was not detected in our dataset, the closely related cis-
6 3,4-methyleneheptanoate was decreased in PD and was the most significantly perturbed
7 branched fatty acid (fold-change = 0.75; FDR = 0.005). Acylcarnitines, which are comprised
8 of fatty acids linked to a carnitine moiety, have important functions in mitochondrial beta-
9 oxidation and have previously been reported to be reduced in blood from individuals with
10 PD^{16,62,63}. For example, we documented PD-associated reductions in cis-3,4-
11 methyleneheptanoylcarnitine (FDR = 0.002), (S)-3-hydroxybutyrylcarnitine (fold-change =
12 0.78, FDR = 0.005), and carnitine itself (fold-change = 0.92, FDR = 0.008). Interestingly, the
13 top-ranked, up-regulated metabolite in PD is an amino acid derivative, hydroxy-N6,N6,N6-
14 trimethyllysine, linked to carnitine synthesis⁶⁴.

15 To determine whether metabolic perturbations are specific for PD, we also analyzed
16 blood from an additional 99 individuals with Alzheimer's disease (AD) (**Supplemental**
17 **Figure 9** and **Supplemental Data 1**). All samples were analyzed together with the PD cases
18 and compared with the same control group. Overall, we identified significant overlap
19 between the differential blood metabolic signatures of AD and PD ($p = 1.8 \times 10^{-8}$)
20 (**Supplemental Figure 9A**). For example, sphingolipid perturbations were also detected in
21 AD, with nine overlapping and concordant metabolites between AD and PD, including two
22 down- and seven up-regulated species (**Supplemental Data 1**). Further, out of the five
23 acylcarnitines down-regulated in PD, only one (carnitine) was also perturbed in AD.

24 Besides lipids, our metabolome-wide analyses also identified PD-specific blood
25 metabolite changes representative of dysregulation in the tricarboxylic acid and urea
26 cycles, as well as altered metabolism of amino acids, polyamines, and nicotinamide
27 metabolism (**Table 2** and **Supplemental Data 1**). On the other hand, potential AD-specific
28 changes included perturbations affecting long chain fatty acids, lysophospholipids,
29 secondary bile acids, and sterols, consistent with findings from other published work⁶⁵⁻⁶⁷.

30 31 A brain acylcarnitine metabolic signature also accompanies preclinical 32 alpha-synuclein pathology

33 We next investigated whether PD metabolic signatures from blood can also be detected in
34 the brain. The diagnosis of PD is preceded by a decades-long, clinically silent phase in
35 which alpha-synuclein brain neuropathology develops in association with absent or

1 minimal motor impairment¹. Therefore, it will be essential to define biomarkers indicating
2 the development and progression of preclinical PD pathophysiology—these markers may
3 also enhance understanding of the causal chain linking the earliest disease triggers to its
4 clinical manifestation. To characterize metabolic changes associated with alpha-synuclein
5 Lewy body pathology, we again leveraged data from ROSMAP²⁹, a prospective study of brain
6 aging that enrolls older adults for longitudinal clinical evaluations with brain autopsy and
7 comprehensive neuropathologic studies following death.

8 Our analysis included a total of 490 brain autopsies (mean age of death = 90.5 years,
9 female = 70.4%), including 129 cases with Lewy body (LB) pathology and 361 controls
10 without LB pathology (**Supplemental Table 2**). Metabolome profiles from postmortem
11 dorsolateral prefrontal cortex tissue were available for analysis ($n = 685$ total metabolites),
12 based on the same comprehensive assay as in our PD clinical cohort with plasma
13 metabolomics. We interrogated for differential metabolite perturbations associated with
14 LB pathology following adjustment for age, sex, and postmortem interval. Overall, only two
15 LB pathology-associated metabolite perturbations met our significance threshold ($FDR <$
16 0.05): N-acetyl-3-methylhistidine and pipecolate (**Supplemental Data 1**). We speculate
17 that metabolic signatures may be rapidly attenuated and potentially obscured due to
18 postmortem artifact, as we noted a strong association between many metabolites and
19 postmortem interval (**Supplemental Data 1**). We therefore focused on more targeted
20 replication of results from blood to brain, applying a suggestive significance threshold
21 (unadjusted $p < 0.05$) for LB-associated metabolic changes. Although there was minimal
22 overlap in the specific metabolites altered across tissues, lipid perturbations accounted
23 for the second largest fraction of suggestive changes detected in LB positive cases (**Figure**
24 **4A and Supplemental Figure 12A**). However, sphingolipids were no longer the dominant
25 signature in the brain, with carnitine and acylcarnitine metabolites instead comprising the
26 most dysregulated category (**Figure 4B**). Further, when considering all acylcarnitines
27 detected by the assay, we found evidence for potential down-regulation among this lipid
28 class in brains, with 28 out of 33 detected species reduced ($p = 1 \times 10^{-5}$).

29 Only 20 of the 129 cases with alpha-synuclein LB pathology included in our analysis
30 carried a PD diagnosis, consistent with a predominantly preclinical or prodromal cohort⁶⁸.
31 In a secondary analysis, we excluded the small number of LB pathology cases with a
32 clinical diagnosis of PD (**Supplemental Data 1**). As expected, the major levodopa
33 breakdown product⁶⁹, 3-methoxytyrosine, which was present in the primary analysis, was
34 no longer detected in this secondary analysis. Interestingly, however, the suggestive
35 acylcarnitine signature was preserved, suggesting that decreases in this class of lipids may
36 accompany PD pathology prior to the manifestation or recognition of the full PD clinical
37 syndrome.

1 2 Alpha-synuclein pathology is associated with a brain proteomic signature 3 suggestive of mitochondrial dysfunction

4 Our results, along with other published work^{13,16–23}, strongly suggest that PD pathology and
5 clinical manifestations are accompanied by altered lipid metabolism, and that certain
6 sphingolipid and fatty acid signatures may mediate the impact of risk genes like *SPTSSB*. To
7 further elaborate the responsible mechanisms for lipid perturbations in PD, we examined
8 differential protein expression in the setting of alpha-synuclein pathology, leveraging
9 available mass-spectrometry proteomics from the same brain autopsy cohort used for
10 metabolomics (93 LB cases and 293 controls) (**Supplemental Figure 12B** and
11 **Supplemental Data 2**).

12 In analyses of single protein differential expression, we did not detect any LB-
13 associated protein perturbations that survive adjustment for multiple testing (FDR < 0.05).
14 Interestingly, the top LB-associated, upregulated protein was midkine (MDK; fold-change =
15 1.27; $p = 0.001$), a secreted growth and immunomodulatory factor, that has also been
16 implicated from AD proteomics^{70,71}. Based on overrepresentation analyses, LB pathology
17 was characterized by a protein expression signature enriched for biological pathways
18 implicated in synaptic structure/function and vesicle trafficking (**Figure 4C** and
19 **Supplemental Data 2**), consistent with a recent published proteomic analysis of
20 postmortem brain tissue from LB dementia⁷². We also noted evidence of enrichment for
21 downregulation of mitochondrial processes, bioenergetics, and fatty acid metabolism.
22 Since acylcarnitines have a critical role in the transport of fatty acids into mitochondria for
23 beta-oxidation²⁵, our complementary metabolomic and proteomic analyses may identify
24 convergent signatures related to mitochondrial dysfunction in PD.

25

26 Discussion

27 A major goal for our field is to understand the molecular cascade from genetic variants to
28 PD pathogenesis, since these pathways may identify causal mechanisms, along with
29 promising biomarkers and targets for disease modifying therapies. *GBA1* and several other
30 risk genes strongly implicate perturbations in sphingolipid/ceramide metabolism in PD
31 pathogenesis^{5–9}. We have integrated genomic, metabolic, transcriptomic, and proteomic
32 data, including from blood and postmortem brain tissue, to probe mechanisms of PD risk
33 and pathogenesis.

1 Building on recent genome-wide association studies, we discovered evidence for a
2 causal chain at the *SPTSSB* susceptibility locus, linking genetic variants, increased mRNA
3 expression, altered sphingolipid and fatty acid levels, and PD risk. *SPTSSB*, encoding a
4 regulatory subunit for the SPT enzyme which catalyzes the initial step in *de novo*
5 sphingolipid biosynthesis, has not been previously studied in PD. SPT condenses a fatty
6 acyl-CoA with serine to create 3-ketosphinganine, which is subsequently modified to form
7 the ceramide backbone for sphingolipids (**Figure 1A**). The trimeric SPT holoenzyme is
8 comprised of 2 large subunits, SPTLC1 and either SPTLC2 or SPTLC3, along with the small
9 regulatory subunit, either SPTSSA or SPTSSB. SPTSSB modifies SPT substrate specificity,
10 favoring the generation of longer chain ceramides^{54,73}. Whereas palmitoyl-CoA produces an
11 18-carbon chain base, which is the most abundant form, alternate substrates, such as
12 stearoyl-CoA or myristoyl-CoA, can lead to longer (C20) or shorter (C16) backbones,
13 respectively, contributing to a diversity of sphingolipid species with varying ceramide
14 backbone lengths⁷⁴. In a naturally occurring gain-of-function mouse mutant, *Stellar*, a
15 single amino acid change in *SPTSSB* (His56Leu) increases the production of longer, C20
16 backbone sphingolipids, leading to intracellular membrane-like inclusions and
17 neurodegeneration⁷⁵. While the causal variant for PD risk remains to be established, the
18 lead variant from published GWAS, *rs1450522*, falls in the *SPTSSB* 5'-UTR, and could
19 potentially impact mRNA turnover. We hypothesize that increased *SPTSSB* expression
20 promotes PD pathogenesis by either increasing overall sphingolipid production and/or
21 favoring the generation of ceramide species with longer base chain lengths, either of which
22 may have a deleterious impact on the central nervous system.

23 *SPTSSB* is expressed in brain, and we confirmed strong colocalization for PD risk
24 variants with *SPTSSB* mRNA expression in excitatory neurons^{5,59}. Whereas *SPTSSB*^{*rs1450522*}
25 showed suggestive associations with increases in several blood ceramide and sphingolipid
26 species, we did not detect similar associations with sphingolipids detected in postmortem
27 brain tissue, nor was this variant related to brain fatty acids or other lipid species. It is
28 possible that larger sample sizes will permit more powerful and direct analyses of brain
29 sphingolipid metabolism; although, the rapid development of postmortem change may
30 obscure metabolic signatures. It is also possible that some of the intermediate species in
31 sphingolipid biosynthesis are short-lived, making them difficult to detect in brain or
32 elsewhere. For example, 3-ketosphinganine the product of SPT, is rapidly transformed to
33 sphinganine *in vivo*⁷⁶. Since *SPTSSB* is poorly expressed in peripheral blood cells^{77,78}, the
34 sphingolipids altered in individuals with the *SPTSSB*^{*rs1450522*} variant may represent spillover
35 from brain sphingolipid pools, or alternatively, could derive from another unknown
36 peripheral tissue source. Common genetic variants at *arylsulfatase A (ARSA)* show
37 associations with both PD risk and reduced levels of O-sulfo-L-tyrosine in cerebrospinal

1 fluid²⁶, and we confirmed that this mQTL is similarly preserved in plasma (**Supplemental**
2 **Figure 8**). We also documented significant colocalization between *SPTSSB* locus variants
3 with PD risk and decreased plasma levels of the fatty acid heptanoate. As discussed
4 further below, although sphingolipid and fatty acid metabolism have multiple plausible
5 connections, additional work will be required to establish whether and how increased
6 *SPTSSB* expression may secondarily trigger depletion of heptanoate or other fatty acids.
7 Notably, the SPT substrate, palmitoyl-CoA, is a key intermediate and modulator for both
8 fatty acid synthesis and breakdown²⁵. Fatty acids are also consumed during the maturation
9 of complex sphingolipids, to generate acyl side chains. Therefore, it is possible that
10 increased SPT activity might indirectly lead to reduced fatty acids; although, other more
11 complex feedback interactions are also possible. Rather than simply a bystander, a
12 decrease in heptanoate, and perhaps other fatty acids, may also influence PD risk /
13 pathogenesis, but additional studies are needed to explore this hypothesis. Heptanoate
14 readily enters the mitochondrion, where it is broken down to acetyl-CoA and propionyl-
15 CoA, driving and sustaining the TCA cycle—a process known as anapleurosis^{79,80}. In fact,
16 the heptanoate triglyceride, triheptanoin—an approved therapy for fatty acid oxidation
17 disorders⁸¹—may also restore brain energy homeostasis and has demonstrated potential
18 benefit in small trials for Huntington’s disease and epilepsy^{82–84}.

19 In our metabolome-wide analysis, we discovered additional evidence for PD
20 associated dysregulation in fatty acid metabolism, with reductions in multiple
21 acylcarnitines observed in both blood and brain. Acylcarnitines mediate the transfer of
22 fatty acids into mitochondria for breakdown via beta-oxidation²⁵. Consistent with this, we
23 found that PD pathology-associated differential protein signatures were significantly
24 enriched for markers of mitochondrial dysfunction, including altered fatty acid
25 metabolism. Based on several independent lines of evidence, mitochondria have long
26 featured centrally in models for PD pathogenesis^{1,85}. Autosomal recessive, juvenile onset
27 PD has been linked to several genes (e.g., *PARKIN/PARK2*) with roles in mitochondrial
28 quality control²⁴. Separately, toxins like rotenone and misfolded alpha-synuclein can
29 similarly target the mitochondrial electron transport chain, promoting oxidative injury as a
30 potential driver for neurodegeneration^{86,87}. The convergent metabolic and proteomic
31 signatures of PD and alpha-synuclein pathology are highly suggestive of altered
32 bioenergetics. Our results also implicate perturbations in the TCA cycle (**Supplemental**
33 **Table 6**), which is not only intimately related to mitochondrial respiration, but also involves
34 key intermediates for both fatty acid and sphingolipid metabolism. The reciprocal
35 interconnection among these metabolic networks is highlighted by experimental
36 manipulations limiting serine bioavailability, which not only profoundly impact
37 sphingolipid/ceramide synthesis (serine is a key substrate for SPT), but also trigger reduced

1 acylcarnitine levels and impaired mitochondrial structure/function, including fatty acid
2 oxidation⁸⁸.

3 Our results add to prior studies highlighting lipid signatures, including
4 sphingolipids¹⁹⁻²¹, fatty acids^{16,22,89}, and fatty acid derivatives like acylcarnitines^{62,63} as
5 promising blood biomarkers for PD. Fewer studies by comparison have also considered
6 postmortem brain tissue, and most of these have been limited by small sample sizes. The
7 autopsy cohort employed here, in which most cases with alpha-synuclein LB pathology are
8 representative of potential early, preclinical PD or Lewy body dementia⁶⁸, is particularly
9 attractive for biomarker discovery. Another strength of our approach comes from the
10 integration of metabolic and genetic data to pinpoint causal pathways. Abundant evidence
11 from human genetics supports a causal pathway from loss-of-function in genes related to
12 ceramide metabolism to PD risk; however, numerous studies also strongly suggest that
13 alpha-synuclein and PD pathophysiology may reciprocally disrupt endosome-lysosomal
14 function, amplifying sphingolipid dysmetabolism^{1,12}. If correct, this bi-directional feedback
15 loop could make it impossible to determine whether metabolic perturbations stem from
16 genetic drivers or rather represent downstream effects of alpha-synuclein pathology. To
17 circumvent this potential confounding, we examined *SPTSSB* variants in neurologically-
18 healthy controls, pinpointing sphingolipid perturbations in individuals at risk for PD but
19 without known pathology. In our complementary analyses of PD cases, *SPTSSB*^{rs1450522} was
20 associated with an increased number of distinct but overlapping subset of sphingolipid
21 metabolites (**Supplemental Table 3**). Notably, prior studies have found glucosylceramide
22 and other sphingolipid changes in *GBA1*-PD cases, but most find that the changes overlap
23 with those seen in idiopathic PD¹⁸. Thus, in future work, it may be important to interrogate
24 metabolism in *GBA1* variant carriers without PD.

25 We note several important study limitations and additional future directions. First,
26 despite interrogation of the plasma metabolome in ~300 PD cases and controls, along with
27 multiple replication/extension datasets with complementary data from blood and brain
28 tissue, it will be essential to replicate our findings in additional independent cohorts.
29 Further, while secondary analyses establish that most of our results are applicable to both
30 males and females with PD, our sample size and composition make it difficult to
31 definitively rule out the potential influence of sex differences in sphingolipid or other
32 metabolic pathways. Third, our data suggests that postmortem interval may be a strong
33 confounder, complicating analyses of the metabolome in brain tissue. Lastly, while the
34 colocalization and SMR results are most consistent with our interpretation of a common
35 causal variant for the associations between *rs1450522* and PD risk, *SPTSSB* expression,
36 and plasma heptanoate levels, we cannot completely exclude alternate causal pathways

1 that violate the instrumental variable assumptions, such as due to pleiotropy or cryptic
2 linkage disequilibrium.

3 In sum, our results highlight promising lipid biomarkers for PD, and in the case of
4 *SPTSSB*, we show how these signatures can aid in the dissection of causal pathways. In the
5 future, it will be important to examine sphingolipids, fatty acids, and acylcarnitines in
6 relation to PD progression, heterogeneity, and therapeutic response. Confirmation of
7 causal lipid signatures for PD risk may further open new therapeutic avenues.

8 Pharmacologic manipulation of lipid metabolism is a well-established therapeutic strategy
9 in cardiovascular disease prevention, making it highly feasible to consider for PD.

10

11 Data availability

12 ROSMAP data is available from the Synapse AD Knowledge Portal
13 (<https://adknowledgeportal.synapse.org>), including bulk brain tissue metabolomics
14 (syn26007830)²⁸, bulk and single-cell RNA-sequencing (syn3505720²⁹, syn53366818)³³,
15 proteomics (syn21449447, syn21448334)⁵¹, and whole genome sequencing
16 (syn11707419)⁵³. ROSMAP clinical, pathologic, and demographic data was obtained from
17 Synapse or requested directly from the Rush Alzheimer's Disease Center. Data from the
18 Surendran et al. metabolome-wide association analysis⁴⁴ is available from
19 (<https://omicscience.org/apps/mgwas/mgwas.table.php>); *SPTSSB* locus summary
20 statistics were provided by Dr. Claudia Langenberg (University of Cambridge). We also
21 downloaded summary statistics from the Cadby et al. lipidome-wide association
22 analysis⁴³. Summary statistics from all BCM-HM data genetic and metabolomic analyses
23 are included with the Supplemental Data Files. Due to privacy concerns and the possible
24 inadvertent release of personal health information, individual-level BCM-HM genetic and
25 metabolomic data are available on request from the corresponding author (JMS).
26 Computational code and pipelines used for data analysis are available in GitHub
27 (https://github.com/ruthbpaula/PD_multiomics/).

28

29 Acknowledgements

30 We thank the patients and others from Baylor College of Medicine and Houston Methodist
31 Hospital who generously participated in our research study. The results published here are
32 in part based on data obtained from the AMP-AD Knowledge Portal

1 (<https://doi.org/10.7303/syn2580853>). Additional data from the Religious Orders Study and
2 Rush Memory and Aging Project were provided by the Rush Alzheimer's Disease Center,
3 Rush University Medical Center, Chicago. We also thank Dr. Claudia Langenberg from the
4 University of Cambridge for sharing data from the Surendran et al. study, and the Global
5 Parkinson's Genetics Program (GP2) for providing GWAS summary statistics. GP2 is funded
6 by the Aligning Science Across Parkinson's (ASAP) initiative and implemented by The
7 Michael J. Fox Foundation for Parkinson's Research (MJFF). For a complete list of GP2
8 investigators, see <https://gp2.org>.

9

10 Funding

11 This work was supported by Huffington Foundation (JMS, CAS), McGee Family Foundation
12 (JMS), Silverstein Foundation for PD with *GBA1* (JMS, JK), the Harrison and Nantz Funds
13 from the Houston Methodist Foundation (JCM), the Jan and Dan Duncan Neurological
14 Research Institute at Texas Children's Hospital (JMS, CAS), and The Effie Marie Caine
15 Endowed Chair for Alzheimer's Research (JMS).

16

17 Competing interests

18 Herve Rhinn and Asa Abeliovich are employed by and have equity ownership in Leal
19 Therapeutics. The other authors report no other competing interests.

20

21 Supplementary material

22 Supplementary Material includes 12 Figures, 7 Tables, and 3 Supplemental Data Files.

23

24 References

- 25 1. Ye H, Robak LA, Yu M, Cykowski M, Shulman JM. Genetics and Pathogenesis of
26 Parkinson's Syndrome. *Annu Rev Pathol.* 2022;18(1). doi:10.1146/ANNUREV-
27 PATHMECHDIS-031521-034145

- 1 2. Bloem BR, Okun MS, Klein C. Parkinson's disease. *The Lancet*.
2 2021;397(10291):2284-2303. doi:10.1016/S0140-6736(21)00218-X
- 3 3. Sidransky E, Nalls MA, Aasly JO, et al. Multicenter analysis of
4 glucocerebrosidase mutations in Parkinson's disease. *N Engl J Med*.
5 2009;361(17):1651-1661. doi:10.1056/NEJMOA0901281
- 6 4. Brady RO, Kanfer JN, Shapiro D. Metabolism of glucocerebrosides II. Evidence
7 of an enzymatic deficiency in Gaucher's disease. *Biochem Biophys Res*
8 *Commun*. 1965;18(2):221-225. doi:10.1016/0006-291X(65)90743-6
- 9 5. Nalls MA, Blauwendraat C, Vallerga CL, et al. Identification of novel risk loci,
10 causal insights, and heritable risk for Parkinson's disease: a meta-analysis of
11 genome-wide association studies. *Lancet Neurol*. 2019;18(12):1091-1102.
12 doi:10.1016/S1474-4422(19)30320-5
- 13 6. Senkevich K, Zorca CE, Dworkind A, et al. GALC variants affect
14 galactosylceramidase enzymatic activity and risk of Parkinson's disease.
15 *Brain*. 2023;146(5):1859-1872. doi:10.1093/BRAIN/AWAC413
- 16 7. Senkevich K, Beletkaia M, Dworkind A, et al. Association of Rare Variants in
17 ARSA with Parkinson's Disease. *Movement Disorders*. 2023;38(10):1806-1812.
18 doi:10.1002/MDS.29521,
- 19 8. Lee JS, Kanai K, Suzuki M, et al. Arylsulfatase A, a genetic modifier of
20 Parkinson's disease, is an α -synuclein chaperone. *Brain*. 2019;142(9):2845-
21 2859. doi:10.1093/BRAIN/AWZ205,
- 22 9. Alcalay RN, Mallett V, Vanderperre B, et al. SMPD1 mutations, activity, and α -
23 synuclein accumulation in Parkinson's disease. *Movement Disorders*.
24 2019;34(4):526-535. doi:10.1002/MDS.27642,
- 25 10. Cuervo AM, Stafanis L, Fredenburg R, Lansbury PT, Sulzer D. Impaired
26 degradation of mutant α -synuclein by chaperone-mediated autophagy.
27 *Science (1979)*. 2004;305(5688):1292-1295. doi:10.1126/SCIENCE.1101738,
- 28 11. Wong YC, Krainc D. α -synuclein toxicity in neurodegeneration: Mechanism and
29 therapeutic strategies. *Nat Med*. 2017;23(2):1-13. doi:10.1038/NM.4269,
- 30 12. Mazzulli JR, Xu YH, Sun Y, et al. Gaucher disease glucocerebrosidase and α -
31 synuclein form a bidirectional pathogenic loop in synucleinopathies. *Cell*.
32 2011;146(1):37-52. doi:10.1016/J.CELL.2011.06.001

- 1 13. Vos M, Klein C, Hicks AA. Role of Ceramides and Sphingolipids in Parkinson's
2 Disease. *J Mol Biol.* 2023;435(12). doi:10.1016/j.jmb.2023.168000
- 3 14. Pan X, Dutta D, Lu S, Bellen HJ. Sphingolipids in neurodegenerative diseases.
4 *Front Neurosci.* 2023;17. doi:10.3389/FNINS.2023.1137893,
- 5 15. Heinzl S, Berg D, Gasser T, Chen H, Yao C, Postuma RB. Update of the MDS
6 research criteria for prodromal Parkinson's disease. *Movement Disorders.*
7 2019;34(10):1464-1470. doi:10.1002/MDS.27802,
- 8 16. Galper J, Dean NJ, Pickford R, et al. Lipid pathway dysfunction is prevalent in
9 patients with Parkinson's disease. *Brain.* 2022;145(10):3472-3487.
10 doi:10.1093/BRAIN/AWAC176
- 11 17. Chen SJ, Chen CC, Liao HY, et al. Association of Fecal and Plasma Levels of
12 Short-Chain Fatty Acids With Gut Microbiota and Clinical Severity in Patients
13 With Parkinson Disease. *Neurology.* 2022;98(8):E848-E858.
14 doi:10.1212/WNL.0000000000013225
- 15 18. Huh YE, Park H, Chiang MSR, et al. Glucosylceramide in cerebrospinal fluid of
16 patients with GBA-associated and idiopathic Parkinson's disease enrolled in
17 PPMI. *NPJ Parkinsons Dis.* 2021;7(1):102. doi:10.1038/S41531-021-00241-3
- 18 19. Blumenreich S, Nehushtan T, Barav OB, et al. Elevation of gangliosides in four
19 brain regions from Parkinson's disease patients with a GBA mutation. *NPJ*
20 *Parkinsons Dis.* 2022;8(1):1-11. doi:10.1038/S41531-022-00363-
21 2;SUBJMETA=320,45,631;KWRD=BIOCHEMISTRY,METABOLOMICS
- 22 20. te Vruchte D, Sturchio A, Priestman DA, et al. Glycosphingolipid Changes in
23 Plasma in Parkinson's Disease Independent of Glucosylceramide Levels. *Mov*
24 *Disord.* 2022;37(10). doi:10.1002/MDS.29163
- 25 21. den Heijer JM, Cullen VC, Pereira DR, et al. A Biomarker Study in Patients with
26 GBA1-Parkinson's Disease and Healthy Controls. *Movement Disorders.*
27 2023;38(5):783-795. doi:10.1002/MDS.29360,
- 28 22. Luo X, Liu Y, Balck A, Klein C, Fleming RMT. Identification of metabolites
29 reproducibly associated with Parkinson's Disease via meta-analysis and
30 computational modelling. *npj Parkinson's Disease* 2024 10:1. 2024;10(1):1-17.
31 doi:10.1038/s41531-024-00732-z

- 1 23. Alcalay RN, Levy OA, Waters CC, et al. Glucocerebrosidase activity in
2 Parkinson's disease with and without GBA mutations. *Brain*. 2015;138(9):2648-
3 2658. doi:10.1093/BRAIN/AWW179,
- 4 24. Narendra DP, Youle RJ. The role of PINK1–Parkin in mitochondrial quality
5 control. *Nat Cell Biol*. 2024;26(10):1639-1651. doi:10.1038/S41556-024-
6 01513-9,
- 7 25. Chandel NS. Lipid metabolism. *Cold Spring Harb Perspect Biol*. 2021;13(9).
8 doi:10.1101/CSHPERSPECT.A040576,
- 9 26. Wang C, Yang C, Western D, et al. Genetic architecture of cerebrospinal fluid
10 and brain metabolite levels and the genetic colocalization of metabolites with
11 human traits. *Nat Genet*. 2024;56(12):2685-2695. doi:10.1038/S41588-024-
12 01973-
13 7;TECHMETA=43,45;SUBJMETA=205,208,2138,375,631,692,699;KWRD=GENO
14 ME-WIDE+ASSOCIATION+STUDIES,NEUROLOGICAL+DISORDERS
- 15 27. Buchman AS, Yu L, Wilson RS, et al. Progressive parkinsonism in older adults is
16 related to the burden of mixed brain pathologies. *Neurology*.
17 2019;92(16):E1821-E1830. doi:10.1212/WNL.0000000000007315,
- 18 28. Batra R, Arnold M, Wörheide MA, et al. The landscape of metabolic brain
19 alterations in Alzheimer's disease. *Alzheimers Dement*. Published online 2022.
20 doi:10.1002/ALZ.12714
- 21 29. Bennett DA, Buchman AS, Boyle PA, Barnes LL, Wilson RS, Schneider JA.
22 Religious Orders Study and Rush Memory and Aging Project. *Journal of*
23 *Alzheimer's Disease*. 2018;64(s1):S161-S189. doi:10.3233/JAD-179939,
- 24 30. Bennett DA, Schneider JA, Bienias JL, Evans DA, Wilson RS. Mild cognitive
25 impairment is related to Alzheimer disease pathology and cerebral infarctions.
26 *Neurology*. 2005;64(5):834-841. doi:10.1212/01.WNL.0000152982.47274.9E
- 27 31. Bennett DA, Schneider JA, Arvanitakis Z, et al. Neuropathology of older
28 persons without cognitive impairment from two community-based studies.
29 *Neurology*. 2006;66(12):1837-1844.
30 doi:10.1212/01.WNL.0000219668.47116.E6
- 31 32. Hyman BT, Trojanowski JQ. Consensus recommendations for the postmortem
32 diagnosis of Alzheimer disease from the National Institute on Aging and the
33 Reagan Institute Working Group on diagnostic criteria for the

- 1 neuropathological assessment of Alzheimer disease. *J Neuropathol Exp*
2 *Neurol.* 1997;56(10):1095-1097. doi:10.1097/00005072-199710000-00002
- 3 33. Mathys H, Boix CA, Akay LA, et al. Single-cell multiregion dissection of
4 Alzheimer's disease. *Nature* 2024 632:8026. 2024;632(8026):858-868.
5 doi:10.1038/s41586-024-07606-7
- 6 34. Hill EJ, Robak LA, Al-Ouran R, et al. Genome Sequencing in the Parkinson
7 Disease Clinic. *Neurol Genet.* 2022;8(4).
8 doi:10.1212/NXG.0000000000200002,
- 9 35. Schneider VA, Graves-Lindsay T, Howe K, et al. Evaluation of GRCh38 and de
10 novo haploid genome assemblies demonstrates the enduring quality of the
11 reference assembly. *Genome Res.* 2017;27(5):849-864.
12 doi:10.1101/GR.213611.116,
- 13 36. Behera S, Catreux S, Rossi M, et al. Comprehensive genome analysis and
14 variant detection at scale using DRAGEN. *Nat Biotechnol.* Published online
15 October 25, 2024:1-15. doi:10.1038/S41587-024-02382-
16 1;SUBJMETA=114,212,61,631,794;KWRD=COMPUTATIONAL+BIOLOGY+AND+
17 BIOINFORMATICS,GENOMICS,SOFTWARE
- 18 37. Mallett V, Ross JP, Alcalay RN, et al. GBA P.T369M substitution in Parkinson
19 disease: Polymorphism or association? A meta-analysis. *Neurol Genet.*
20 2016;2(5). doi:10.1212/NXG.0000000000000104,
- 21 38. Goldstein O, Gana-Weisz M, Cohen-Avinoam D, et al. Revisiting the non-
22 Gaucher-GBA-E326K carrier state: Is it sufficient to increase Parkinson's
23 disease risk? *Mol Genet Metab.* 2019;128(4):470-475.
24 doi:10.1016/J.YMGME.2019.10.001
- 25 39. Chong J, Soufan O, Li C, et al. MetaboAnalyst 4.0: towards more transparent
26 and integrative metabolomics analysis. *Nucleic Acids Res.*
27 2018;46(W1):W486-W494. doi:10.1093/NAR/GKY310
- 28 40. R Core Team. R: A Language and Environment for Statistical Computing.
29 Preprint posted online 2021. <https://www.R-project.org/>
- 30 41. Wickham H. *Ggplot2: Elegant Graphics for Data Analysis*. Springer-Verlag New
31 York; 2016. <https://ggplot2.tidyverse.org>

- 1 42. Sekhon JS. Multivariate and propensity score matching software with
2 automated balance optimization: The matching package for R. *J Stat Softw.*
3 2011;42(7):1-52. doi:10.18637/JSS.V042.I07
- 4 43. Cadby G, Giles C, Melton PE, et al. Comprehensive genetic analysis of the
5 human lipidome identifies loci associated with lipid homeostasis with links to
6 coronary artery disease. *Nat Commun.* 2022;13(1):3124. doi:10.1038/S41467-
7 022-30875-7
- 8 44. Surendran P, Stewart ID, Au Yeung VPW, et al. Rare and common genetic
9 determinants of metabolic individuality and their effects on human health.
10 *Nature Medicine* 2022 28:11. 2022;28(11):2321-2332. doi:10.1038/s41591-
11 022-02046-0
- 12 45. Giambartolomei C, Vukcevic D, Schadt EE, et al. Bayesian Test for
13 Colocalisation between Pairs of Genetic Association Studies Using Summary
14 Statistics. *PLoS Genet.* 2014;10(5):e1004383.
15 doi:10.1371/JOURNAL.PGEN.1004383
- 16 46. GALC/coloc at main · gan-orlab/GALC · GitHub. Accessed June 16, 2025.
17 <https://github.com/gan-orlab/GALC/blob/main/coloc>
- 18 47. (GP2) TGPGP, Leonard HL. Novel Parkinson's Disease Genetic Risk Factors
19 Within and Across European Populations. *medRxiv.* Published online March
20 17, 2025:2025.03.14.24319455. doi:10.1101/2025.03.14.24319455
- 21 48. Lonsdale J, Thomas J, Salvatore M, et al. The Genotype-Tissue Expression
22 (GTEx) project. *Nature Genetics* 2013 45:6. 2013;45(6):580-585.
23 doi:10.1038/ng.2653
- 24 49. Zhu Z, Zhang F, Hu H, et al. Integration of summary data from GWAS and eQTL
25 studies predicts complex trait gene targets. *Nature Genetics* 2016 48:5.
26 2016;48(5):481-487. doi:10.1038/ng.3538
- 27 50. Rare and common genetic determinants of metabolic individuality and their
28 effects on human health. Accessed June 16, 2025.
29 <https://omicscience.org/apps/mgwas/mgwas.table.php>
- 30 51. Johnson ECB, Carter EK, Dammer EB, et al. Large-scale deep multi-layer
31 analysis of Alzheimer's disease brain reveals strong proteomic disease-related
32 changes not observed at the RNA level. *Nature Neuroscience* 2022 25:2.
33 2022;25(2):213-225. doi:10.1038/s41593-021-00999-y

- 1 52. Zhou Y, Zhou B, Pache L, et al. Metascape provides a biologist-oriented
2 resource for the analysis of systems-level datasets. *Nat Commun.* 2019;10(1).
3 doi:10.1038/S41467-019-09234-6,
- 4 53. Vialle RA, de Paiva Lopes K, Bennett DA, Crary JF, Raj T. Integrating whole-
5 genome sequencing with multi-omic data reveals the impact of structural
6 variants on gene regulation in the human brain. *Nat Neurosci.* 2022;25(4):504.
7 doi:10.1038/S41593-022-01031-7
- 8 54. Santos TCB, Dingjan T, Futerman AH. The sphingolipid anteome: implications
9 for evolution of the sphingolipid metabolic pathway. *FEBS Lett.*
10 2022;596(18):2345-2363. doi:10.1002/1873-3468.14457,
- 11 55. Srivastava S, Shaked HM, Gable K, et al. SPTSSA variants alter sphingolipid
12 synthesis and cause a complex hereditary spastic paraplegia. *Brain.*
13 2023;146(4):1420-1435. doi:10.1093/BRAIN/AWAC460
- 14 56. Naruse H, Ishiura H, Esaki K, et al. SPTLC2 variants are associated with early-
15 onset ALS and FTD due to aberrant sphingolipid synthesis. *Ann Clin Transl*
16 *Neurol.* 2024;11(4):946-957. doi:10.1002/ACN3.52013,
- 17 57. Dohrn MF, Beijer D, Lone MA, et al. Recurrent de-novo gain-of-function
18 mutation in SPTLC2 confirms dysregulated sphingolipid production to cause
19 juvenile amyotrophic lateral sclerosis. *J Neurol Neurosurg Psychiatry.*
20 2023;95(3):201-205. doi:10.1136/JNNP-2023-332130,
- 21 58. Syeda SB, Lone MA, Mohassel P, et al. Recurrent de novo SPTLC2 variant
22 causes childhood-onset amyotrophic lateral sclerosis (ALS) by excess
23 sphingolipid synthesis. *J Neurol Neurosurg Psychiatry.* 2023;95(2):103-113.
24 doi:10.1136/JNNP-2023-332132,
- 25 59. Bryois J, Calini D, Macnair W, et al. Cell-type-specific cis-eQTLs in eight human
26 brain cell types identify novel risk genes for psychiatric and neurological
27 disorders. *Nat Neurosci.* 2022;25(8):1104-1112. doi:10.1038/S41593-022-
28 01128-Z,
- 29 60. Ng B, White CC, Klein HU, et al. An xQTL map integrates the genetic
30 architecture of the human brain's transcriptome and epigenome. *Nat*
31 *Neurosci.* 2017;20(10):1418-1426. doi:10.1038/NN.4632
- 32 61. Li YI, Wong G, Humphrey J, Raj T. Prioritizing Parkinson's disease genes using
33 population-scale transcriptomic data. *Nature Communications* 2019 10:1.
34 2019;10(1):1-10. doi:10.1038/s41467-019-08912-9

- 1 62. Shao Y, Li T, Liu Z, et al. Comprehensive metabolic profiling of Parkinson's
2 disease by liquid chromatography-mass spectrometry. *Mol Neurodegener.*
3 2021;16(1):1-15. doi:10.1186/S13024-021-00425-8/FIGURES/6
- 4 63. Saiki S, Hatano T, Fujimaki M, et al. Decreased long-chain acylcarnitines from
5 insufficient β -oxidation as potential early diagnostic markers for Parkinson's
6 disease. *Sci Rep.* 2017;7(1):1-15. doi:10.1038/S41598-017-06767-
7 Y/FIGURES/5
- 8 64. Steiber A, Kerner J, Hoppel CL. Carnitine: A nutritional, biosynthetic, and
9 functional perspective. *Mol Aspects Med.* 2004;25(5-6):455-473.
10 doi:10.1016/j.mam.2004.06.006
- 11 65. Wong MW, Braidy N, Poljak A, Pickford R, Thambisetty M, Sachdev PS.
12 Dysregulation of lipids in Alzheimer's disease and their role as potential
13 biomarkers. *Alzheimer's and Dementia.* 2017;13(7):810-827.
14 doi:10.1016/J.JALZ.2017.01.008,
- 15 66. Varma VR, Oommen AM, Varma S, et al. Brain and blood metabolite signatures
16 of pathology and progression in Alzheimer disease: A targeted metabolomics
17 study. *PLoS Med.* 2018;15(1). doi:10.1371/JOURNAL.PMED.1002482,
- 18 67. Horgusluoglu E, Neff R, Song WM, et al. Integrative metabolomics-genomics
19 approach reveals key metabolic pathways and regulators of Alzheimer's
20 disease. *Alzheimer's and Dementia.* 2022;18(6):1260-1278.
21 doi:10.1002/ALZ.12468,
- 22 68. Buchman AS, Shulman JM, Nag S, et al. Nigral pathology and parkinsonian
23 signs in elders without Parkinson disease. *Ann Neurol.* 2012;71(2):258-266.
24 doi:10.1002/ANA.22588,
- 25 69. Pappan KL, Kennedy AD, Magoulas PL, Hanchard NA, Sun Q, Elsea SH. Clinical
26 Metabolomics to Segregate Aromatic Amino Acid Decarboxylase Deficiency
27 From Drug-Induced Metabolite Elevations. *Pediatr Neurol.* 2017;75:66-72.
28 doi:10.1016/J.PEDIATRNEUROL.2017.06.014
- 29 70. Neumaier EE, Rothhammer V, Linnerbauer M. The role of midkine in health and
30 disease. *Front Immunol.* 2023;14:1310094. doi:10.3389/FIMMU.2023.1310094
- 31 71. Levites Y, Dammer EB, Ran Y, et al. Integrative proteomics identifies a
32 conserved A β amyloid response, novel plaque proteins, and pathology
33 modifiers in Alzheimer's disease. *Cell Rep Med.* 2024;5(8).
34 doi:10.1016/j.xcrm.2024.101669

- 1 72. Shantaraman A, Dammer EB, Ugochukwu O, et al. Network proteomics of the
2 Lewy body dementia brain reveals presynaptic signatures distinct from
3 Alzheimer's disease. *Mol Neurodegener.* 2024;19(1):1-24.
4 doi:10.1186/S13024-024-00749-1/FIGURES/1
- 5 73. Han G, Gupta SD, Gable K, et al. Identification of small subunits of
6 mammalian serine palmitoyltransferase that confer distinct acyl-CoA
7 substrate specificities. *Proc Natl Acad Sci U S A.* 2009;106(20):8186-8191.
8 doi:10.1073/PNAS.0811269106,
- 9 74. Glueck M, Lucaciu A, Subburayalu J, et al. Atypical sphingosine-1-phosphate
10 metabolites—biological implications of alkyl chain length. *Pflugers Arch.*
11 2024;476(12):1833-1843. doi:10.1007/S00424-024-03018-8/METRICS
- 12 75. Zhao L, Spassieva S, Gable K, et al. Elevation of 20-carbon long chain bases
13 due to a mutation in serine palmitoyltransferase small subunit b results in
14 neurodegeneration. *Proc Natl Acad Sci U S A.* 2015;112(42):12962-12967.
15 doi:10.1073/PNAS.1516733112
- 16 76. Lone MA, Santos T, Alecu I, Silva LC, Hornemann T. 1-Deoxysphingolipids.
17 *Biochimica et Biophysica Acta (BBA) - Molecular and Cell Biology of Lipids.*
18 2019;1864(4):512-521. doi:10.1016/J.BBALIP.2018.12.013
- 19 77. SPTSSB protein expression summary - The Human Protein Atlas. Accessed
20 June 16, 2025. <https://www.proteinatlas.org/ENSG00000196542-SPTSSB>
- 21 78. Aguet F, Barbeira AN, Bonazzola R, et al. The GTEx Consortium atlas of genetic
22 regulatory effects across human tissues. *Science (1979).*
23 2020;369(6509):1318-1330.
24 doi:10.1126/SCIENCE.AAZ1776/SUPPL_FILE/AAZ1776_TABLESS10-S16.XLSX
- 25 79. Marin-Valencia I, Good LB, Ma Q, Malloy CR, Pascual JM. Heptanoate as a
26 neural fuel: Energetic and neurotransmitter precursors in normal and glucose
27 transporter I-deficient (G1D) brain. *Journal of Cerebral Blood Flow and*
28 *Metabolism.* 2013;33(2):175-182.
29 doi:10.1038/JCBFM.2012.151/SUPPL_FILE/JCBFM2012151X2.DOC
- 30 80. Inigo M, Deja S, Burgess SC. Ins and Outs of the TCA Cycle: The Central Role of
31 Anaplerosis. *Annu Rev Nutr.* 2021;41:19-47. doi:10.1146/ANNUREV-NUTR-
32 120420-025558
- 33 81. Gillingham MB, Heitner SB, Martin J, et al. Triheptanoin versus trioctanoin for
34 long-chain fatty acid oxidation disorders: a double blinded, randomized

- 1 controlled trial. *J Inherit Metab Dis.* 2017;40(6):831-843. doi:10.1007/S10545-
2 017-0085-8
- 3 82. Mochel F. Triheptanoin for the treatment of brain energy deficit: A 14-year
4 experience. *J Neurosci Res.* 2017;95(11):2236-2243. doi:10.1002/JNR.24111
- 5 83. Mochel F, Méneret A, Adanyeguh IM, et al. Effect of Triheptanoin on Caudate
6 Atrophy and Motor Scores in Patients With Early-Stage Huntington Disease: A
7 Phase II Study. *Neurology.* 2025;104(2). doi:10.1212/WNL.0000000000210194
- 8 84. Striano P, Auvin S, Collins A, et al. A randomized, double-blind trial of
9 triheptanoin for drug-resistant epilepsy in glucose transporter 1 deficiency
10 syndrome. *Epilepsia.* 2022;63(7):1748-1760. doi:10.1111/EPI.17263
- 11 85. Malpartida AB, Williamson M, Narendra DP, Wade-Martins R, Ryan BJ.
12 Mitochondrial Dysfunction and Mitophagy in Parkinson's Disease: From
13 Mechanism to Therapy. *Trends Biochem Sci.* 2021;46(4):329-343.
14 doi:10.1016/j.tibs.2020.11.007
- 15 86. Chung E, Choi Y, Park J, et al. Intracellular delivery of Parkin rescues neurons
16 from accumulation of damaged mitochondria and pathological α -synuclein.
17 *Sci Adv.* 2020;6(18). doi:10.1126/SCIADV.ABA1193,
- 18 87. McKnight S, Hack N. Toxin-Induced Parkinsonism. *Neurol Clin.*
19 2020;38(4):853-865. doi:10.1016/j.ncl.2020.08.003
- 20 88. Gao X, Lee K, Reid MA, et al. Serine Availability Influences Mitochondrial
21 Dynamics and Function through Lipid Metabolism. *Cell Rep.*
22 2018;22(13):3507-3520.
23 doi:10.1016/J.CELREP.2018.03.017/ATTACHMENT/2C5C1E4B-E744-4FD8-
24 9C41-B6439A3B21FE/MMC2.PDF
- 25 89. Fanning S, Selkoe D. Parkinson disease is a fatty acidopathy. *Nat Rev Neurol.*
26 2025;21(11). doi:10.1038/S41582-025-01142-2

27
28
29
30

1 Figure legends

2

3 **Figure 1 Sphingolipid perturbations in Parkinson's disease (PD) cases and genetically**
 4 **at-risk controls.** (A) Schematic showing the *de novo* sphingolipid synthesis and selected
 5 related metabolic pathways. PD risk genes are denoted in green. (B) Boxplots show
 6 representative sphingolipid perturbations in 149 PD cases versus 150 controls. Normalized
 7 residuals (z-scores) are plotted, following adjustment for age and sex. Significance testing
 8 was based on the likelihood ratio test and a false discovery rate (FDR) for multiple testing
 9 (q-value). The following sphingolipids are shown: Dihydroceramide = N-stearoyl-
 10 sphinganine (d18:0/18:0), Glucosylceramide = glycosyl ceramide (d18:1/23:1, d17:1/24:1),
 11 Lactosylceramide = lactosyl-N-nervonoyl-sphingosine (d18:1/24:1), Sphingomyelin =
 12 sphingomyelin (d18:2/24:1, d18:1/24:2). (C) Among 150 controls without PD, boxplots
 13 show sphingolipid increases in heterozygous (Het) or homozygous (Hom) carriers of the PD
 14 risk variant, *rs1450522*, at the *SPTSSB* locus when compared with non-carriers (NC). The
 15 whiskers denote the interquartile range between the first and third quartiles. Normalized
 16 residuals (z-scores) are plotted, following adjustment for age and sex. Significance testing
 17 was based on logistic regression considering an additive inheritance model, except for
 18 glucosylceramide, where a recessive model was employed. Unadjusted p-values are
 19 indicated: *, $p < 0.05$; ***, $p < 0.005$. The following sphingomyelins are shown: (i)
 20 sphingomyelin (d18:1/22:1, d18:2/22:0, d16:1/24:1), (ii) sphingomyelin (d18:2/23:0,
 21 d18:1/23:1, d17:1/24:1), (iii) sphingomyelin (d18:2/21:0, d16:2/23:0), (iv) sphingomyelin
 22 (d18:2/24:1, d18:1/24:2), (v) sphingomyelin (d18:1/20:0, d16:1/22:0), (vi) sphingomyelin
 23 (d18:2/24:2). Glucosylceramide = glycosyl ceramide (d18:1/23:1, d17:1/24:1),
 24 Lactosylceramide = lactosyl-N-nervonoyl-sphingosine (d18:1/24:1). (D) Volcano plot
 25 showing lipid metabolites associated with *rs1450522* meeting the suggestive significance
 26 threshold (unadjusted $p < 0.05$ dashed horizontal line), with sphingolipids highlighted in
 27 red. A total of 629 lipid species were interrogated in $n = 4,492$ individuals without known
 28 neurological disease⁴³. See also Table S3, Figures S3-5, and Supplemental Data File 3.

29

30 **Figure 2 Parkinson's disease (PD) risk variants at the *SPTSSB* locus co-localize with**
 31 ***SPTSSB* mRNA expression and fatty acid metabolism.** (A) Hypothetical causal chain
 32 linking genetic variation at the *SPTSSB* gene with PD risk. (B) At left, locus plots
 33 (chromosome position versus p-value) show variant associations at the *SPTSSB* locus with
 34 PD risk (top, GP2 GWAS data), *SPTSSB* mRNA (middle, eQTL from ROSMAP excitatory
 35 neurons), or plasma heptanoate levels (bottom, mQTL from Surendran et al., 2022). At
 36 right, co-localization plots show causal relationships keyed to numbering in panel A.

1 Significance testing based on posterior probability, PP.H4, denoting the likelihood that both
2 traits share a common causal variant (PP.H4 > 0.8 was considered significant). Color key
3 denotes linkage disequilibrium (LD) of each variant with *rs1450522*. See also Figures S1,
4 S6-7, Table S4, S5, and Supplementary Data File 3.

5
6 **Figure 3 Parkinson's disease (PD) is characterized by lipid metabolic perturbations in**
7 **blood.** Differential metabolism was assessed in plasma from 149 PD cases and 150
8 controls without PD, using the likelihood ratio test and adjusting for age and sex. (A)
9 Volcano plots show up- (red) or down-regulated (blue) meeting the significance threshold
10 defined by a false discovery rate (FDR) q -value < 0.05 (dashed horizontal line). At left, the
11 full plot is notable for extreme perturbations in levodopa metabolites. At right, these outlier
12 values are excluded to magnify the boxed region. Lipid species are denoted with larger,
13 darker dots. (B) Plots showing the total with number of dysregulated species in PD, broken
14 down by metabolite class. Up- and down-regulated, denoted by red and blue color,
15 respectively. (D) Plots showing the proportion (%) of dysregulated species within each lipid
16 class, with up- (red) and down- (blue) regulated changes indicated. The sphingolipid and
17 other lipid classes were significantly enriched for dysregulated metabolites, based on a
18 Fisher test $p < 0.05$. See also Table 2 and Figure S2, and Supplemental Data File 1.

19
20 **Figure 4 Alpha-synuclein Lewy body (LB) pathology is characterized by an acylcarnitine**
21 **metabolic signature and differential expression of mitochondrial proteins.** Differential
22 metabolism and protein expression were interrogated in ROSMAP postmortem brain tissue
23 (dorsolateral prefrontal cortex) data including 129 cases with LB pathology and 361
24 controls without LB pathology, using the likelihood ratio test and adjusting for age and sex.
25 Plots showing the number (A) and proportion (B) of dysregulated species associated with
26 LB pathology, broken down by metabolite class. Up- and down-regulated, denoted by red
27 and blue color, respectively. The carnitine/acylcarnitine class was significantly enriched for
28 dysregulated metabolites, based on a Fisher test $p < 0.05$. (C) Plot showing results of
29 pathway enrichment analysis from differential protein expression in LB pathology, including
30 top-ranked pathways (top) and mitochondrial pathways (bottom). The proportion (%) of
31 differential expressed proteins from pathway is noted, with up- (red) and down- (blue)
32 regulated changes indicated (%). All displayed pathways were significantly enriched, based
33 on Fisher test (false discovery rate adjusted $p < 0.05$). See also Figure S12, Table S6, and
34 Supplemental Data File 2.

35

1

Table 1 Summary-based-Mendelian randomization at the SPTSSB locus

| Exposure | Outcome | Effect | SE | P_{single} | P_{multi} | P_{HEIDI} |
|----------------------------------|--------------------------|--------|------|------------------------|------------------------|-------------|
| SPTSSB eQTL (excitatory neurons) | PD | 0.24 | 0.04 | 1.94×10^{-10} | 1.94×10^{-10} | 0.59 |
| heptanoate mQTL (plasma) | PD | -1.82 | 0.53 | 5.71×10^{-4} | 5.71×10^{-4} | 0.52 |
| SPTSSB eQTL (excitatory neurons) | Heptanoate mQTL (plasma) | -0.12 | 0.03 | 5.32×10^{-4} | 3.54×10^{-3} | 0.30 |

Summary-based Mendelian randomization (SMR) significance based on single and multi-SNP (multi) $p < 0.05$, and HEIDI $p > 0.05$ to confirm the absence of pleiotropy.

2
3
4
5**Table 2 Representative perturbed metabolites in PD plasma**

| Class | Pathway | Metabolite ^a | Fold-change | FDR ^b |
|----------------------|--|--|-------------|------------------------|
| Amino Acids | Glutamate | N-acetylglutamine | 1.26 | 1.37×10^{-3} |
| | Glutathione | 2-hydroxybutyrate/2-hydroxyisobutyrate | 0.80 | 8.99×10^{-3} |
| | Glycine, Serine & Threonine | N-acetylglycine | 1.55 | 4.17×10^{-5} |
| | Histidine | hydantoin-5-propionate | 0.73 | 4.97×10^{-3} |
| | Lactoyl Amino Acid | N-lactoyl-tyrosine | 0.23 | 9.73×10^{-45} |
| | Leucine, Isoleucine & Valine | 2-hydroxy-3-methylvalerate | 1.23 | 7.79×10^{-3} |
| | Lysine | hydroxy-N6,N6,N6-trimethyllysine | 1.84 | 7.46×10^{-22} |
| | Methionine, Cysteine, & SAM | 2-hydroxy-4-(methylthio)butanoic acid | 1.32 | 4.17×10^{-4} |
| | Phenylalanine | phenyllactate (PLA) | 1.32 | 3.92×10^{-5} |
| | Polyamine | acisoga | 0.53 | 9.55×10^{-14} |
| | Tryptophan | indoleacetate | 0.59 | 4.27×10^{-9} |
| | Tyrosine | 3-methoxytyrosine | 107.62 | 2.02×10^{-89} |
| | Urea cycle; Arginine & Proline | homoarginine | 0.77 | 1.76×10^{-6} |
| Cofactors & Vitamins | Ascorbate & Aldarate | 2-O-methylascorbic acid | 0.79 | 6.90×10^{-4} |
| | Nicotinate & Nicotinamide | trigonelline (N'-methylnicotinate) | 0.59 | 1.13×10^{-3} |
| Energy | TCA Cycle | citraconate/glutaconate* | 0.54 | 1.52×10^{-3} |
| Lipids | Carnitine | carnitine* | 0.92 | 7.95×10^{-3} |
| | Dihydroceramides | N-stearoyl-sphinganine (d18:0/18:0) | 0.57 | 7.44×10^{-6} |
| | Dihydrosphingomyelins | behenoyl dihydrosphingomyelin (d18:0/22:0)* | 0.71 | 2.05×10^{-9} |
| | Fatty Acids (Acyl Carnitine, Hydroxy) | (S)-3-hydroxybutyrylcarnitine | 0.78 | 4.83×10^{-3} |
| | Fatty Acids (Acyl Carnitine, Medium Chain) | cis-3,4-methyleneheptanoylcarnitine | 0.79 | 2.02×10^{-3} |
| | Fatty Acid (also BCAA Metabolism) | propionylglycine | 1.62 | 4.71×10^{-4} |
| | Fatty Acid, Amino | N-acetyl-2-aminooctanoate | 0.68 | 2.01×10^{-6} |
| | Fatty Acid, Branched | cis-3,4-methyleneheptanoate | 0.75 | 4.95×10^{-3} |
| | Fatty Acid, Dicarboxylate | maleate* | 0.71 | 1.21×10^{-3} |
| | Fatty Acid, Dihydroxy | 2R,3R-dihydroxybutyrate | 0.81 | 5.74×10^{-4} |
| | Hexosylceramides | glucosyl-N-behenoyl-sphingadienine (d18:2/22:0)* | 1.19 | 6.96×10^{-3} |
| | Lactosylceramides | lactosyl-N-nervonoyl-sphingosine (d18:1/24:1)* | 1.15 | 3.78×10^{-3} |
| | Sphingomyelins | sphingomyelin (d18:1/25:0, d19:0/24:1, d20:1/23:0, d19:1/24:0) | 0.83 | 4.70×10^{-3} |
| Nucleotides | Purine, (Hypo)Xanthine/Inosine | inosine | 1.33 | 6.26×10^{-4} |
| Other | - | bilirubin degradation product, C17H18N2O4 (2) | 0.76 | 8.36×10^{-4} |
| Peptides | Dipeptide | cyclo(leu-pro)* | 0.57 | 5.34×10^{-6} |
| | Gamma-glutamyl Amino Acid | gamma-glutamylglycine | 1.21 | 5.29×10^{-5} |

^aSelected, top-ranked perturbed metabolites in PD plasma for each pathway is shown. Metabolites that are also perturbed in AD plasma are indicated with asterisk (*).

^bFalse Discovery Rate (FDR) adjusted q-values are shown based on likelihood ratio test, adjusted for age and sex.

6
7
8
9

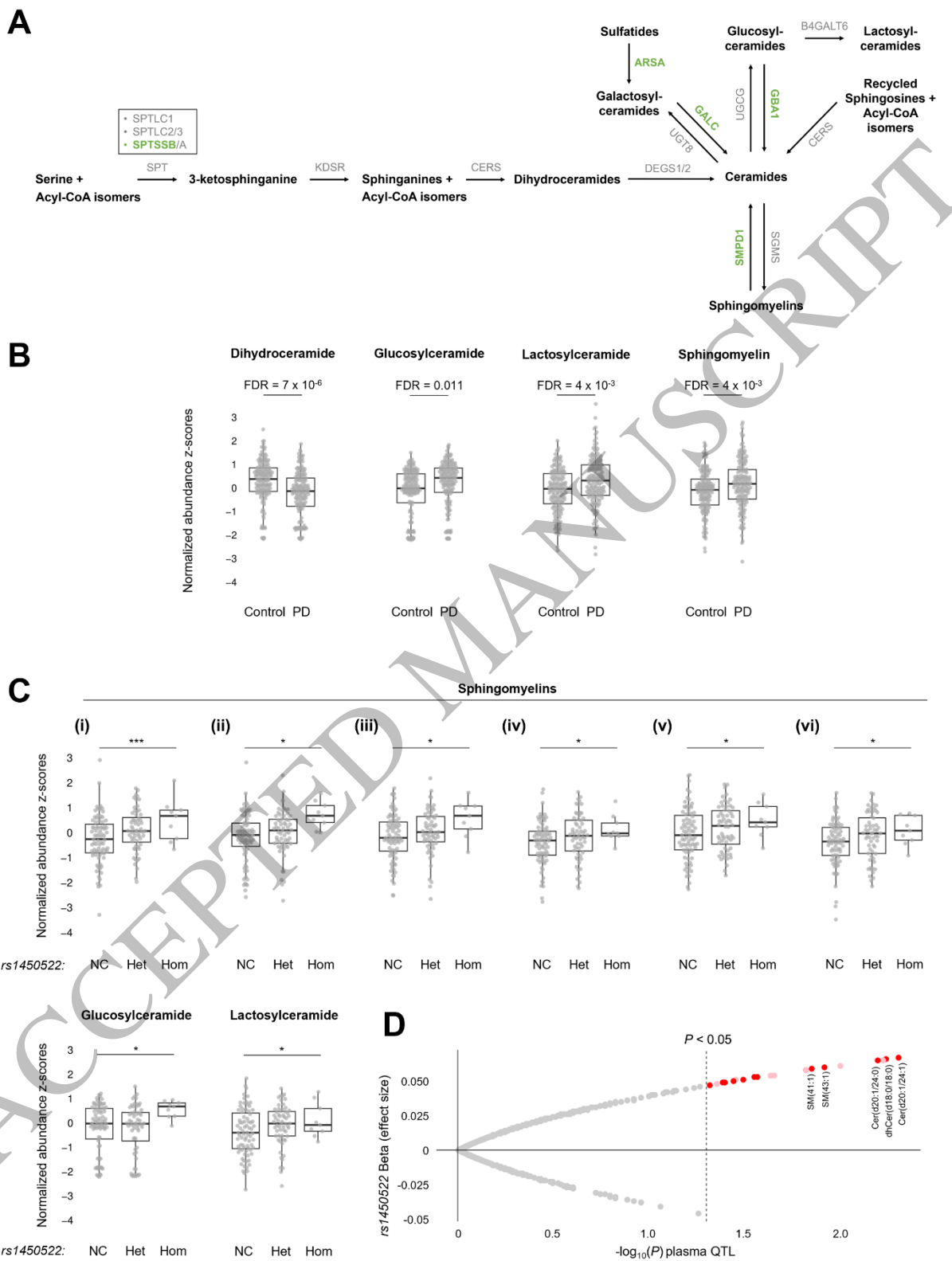


Figure 1
165x212 mm (DPI)

1
2
3

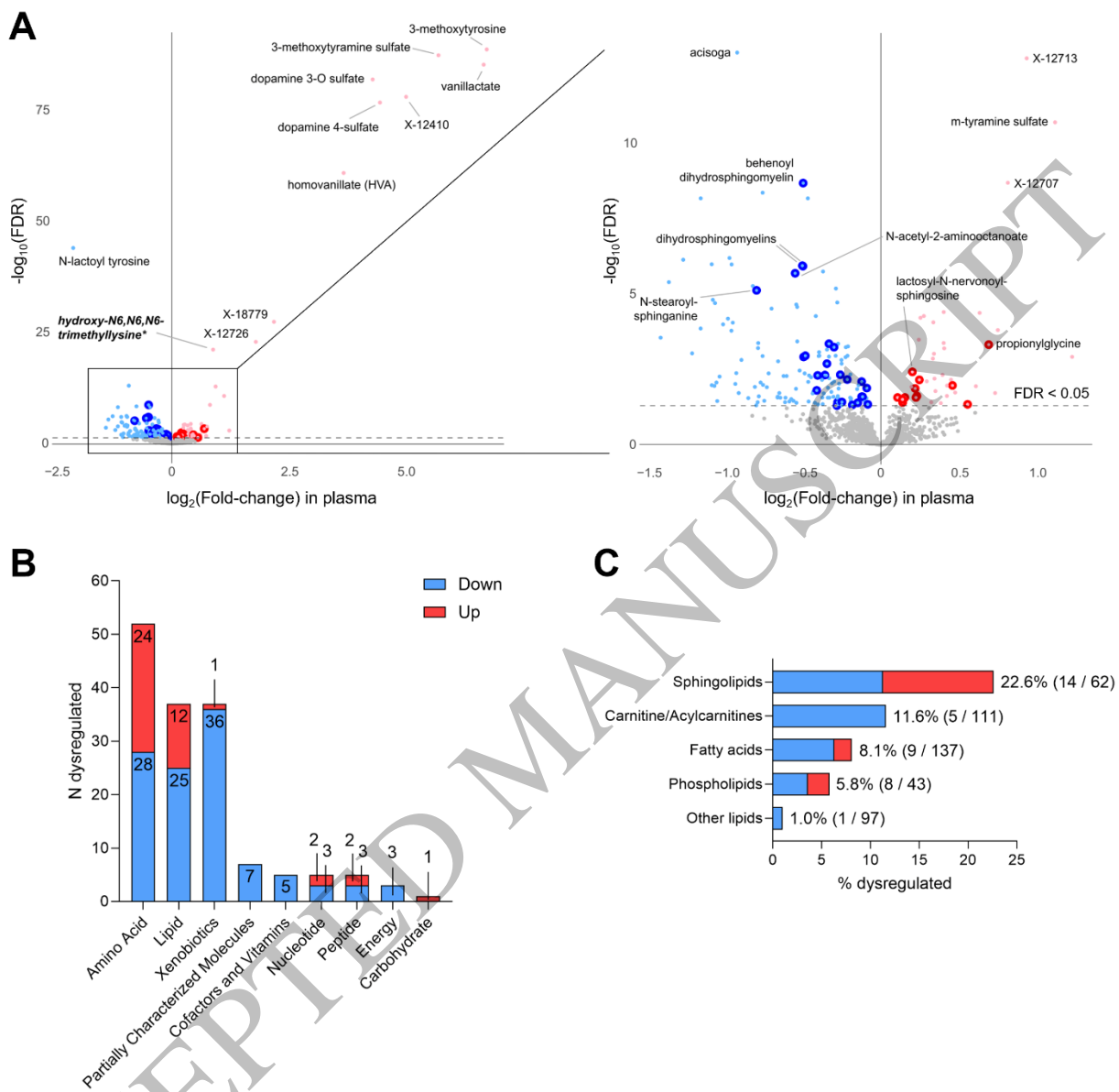


Figure 3
165x161 mm (DPI)

1
2
3
4

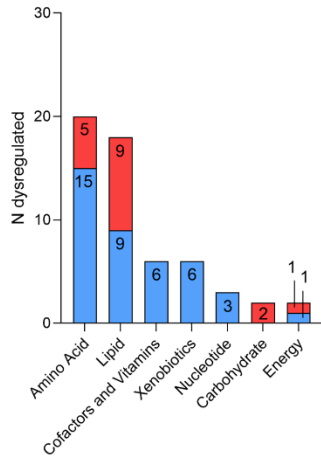
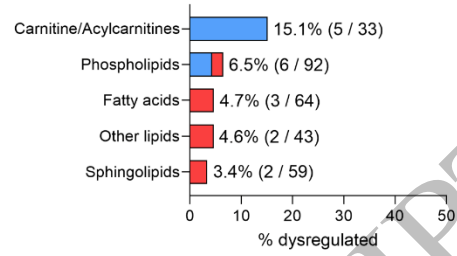
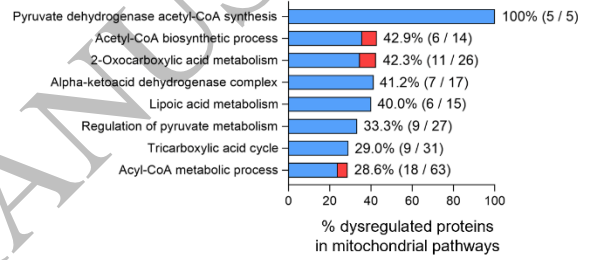
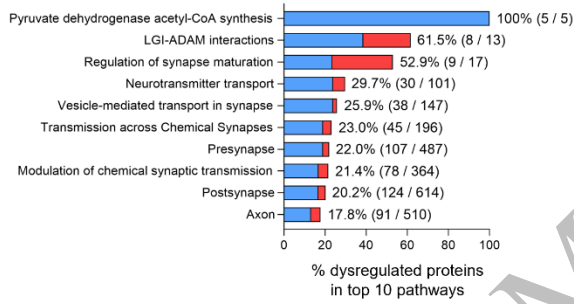
A**B****C**

Figure 4
165x116 mm (DPI)

1
2
3